Supplement of

The sources and diurnal variations of submicron aerosols in a coastal-rural environment near Houston, US

Jing Li et al.

Correspondence to: Jian Wang (jian@wustl.edu) or Lu Xu (xu1@wustl.edu)

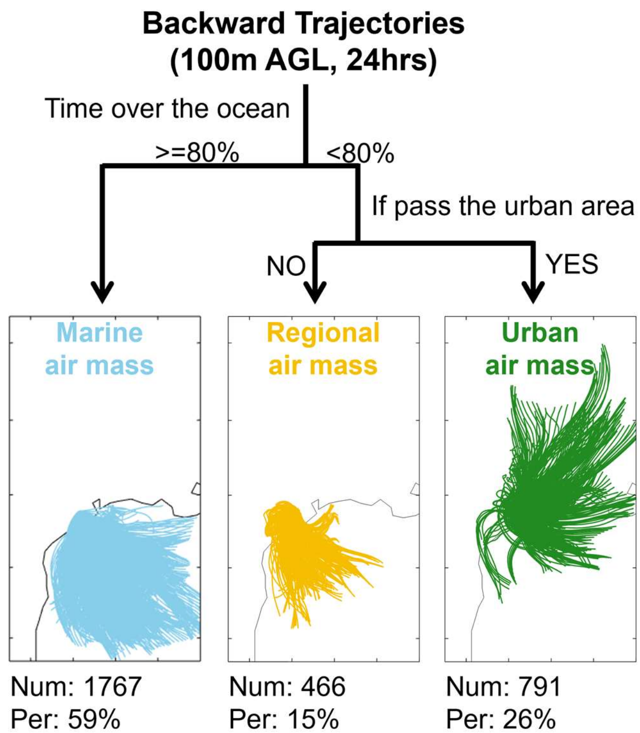

Figure S1. Criteria of the air masses classification.

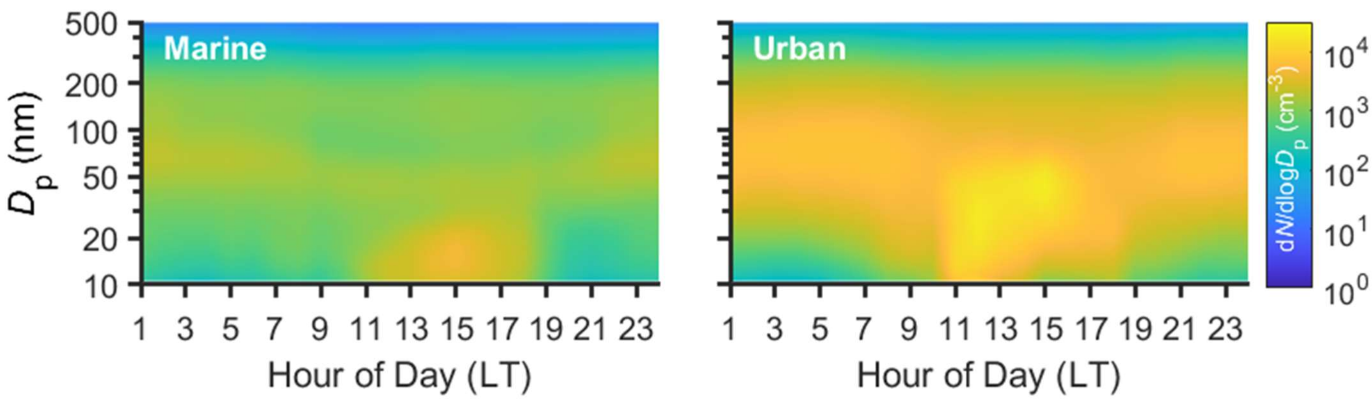

Figure S2. Diurnal variations of particle size distributions in marine and urban air masses observed at the ANC site during the IOP.

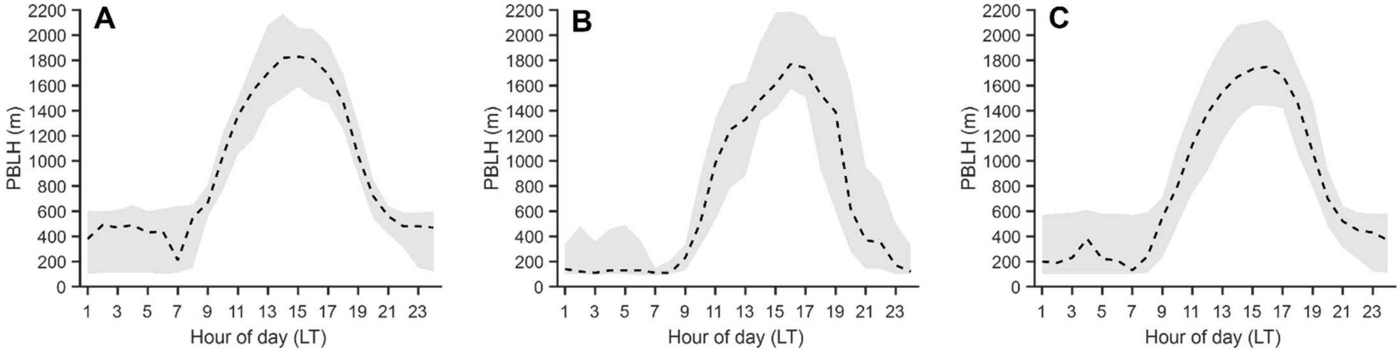

Figure S3. Diurnal variations of planetary boundary layer height (PBLH) of (A) marine, (B) urban, and (C) unseparated (all) air masses.

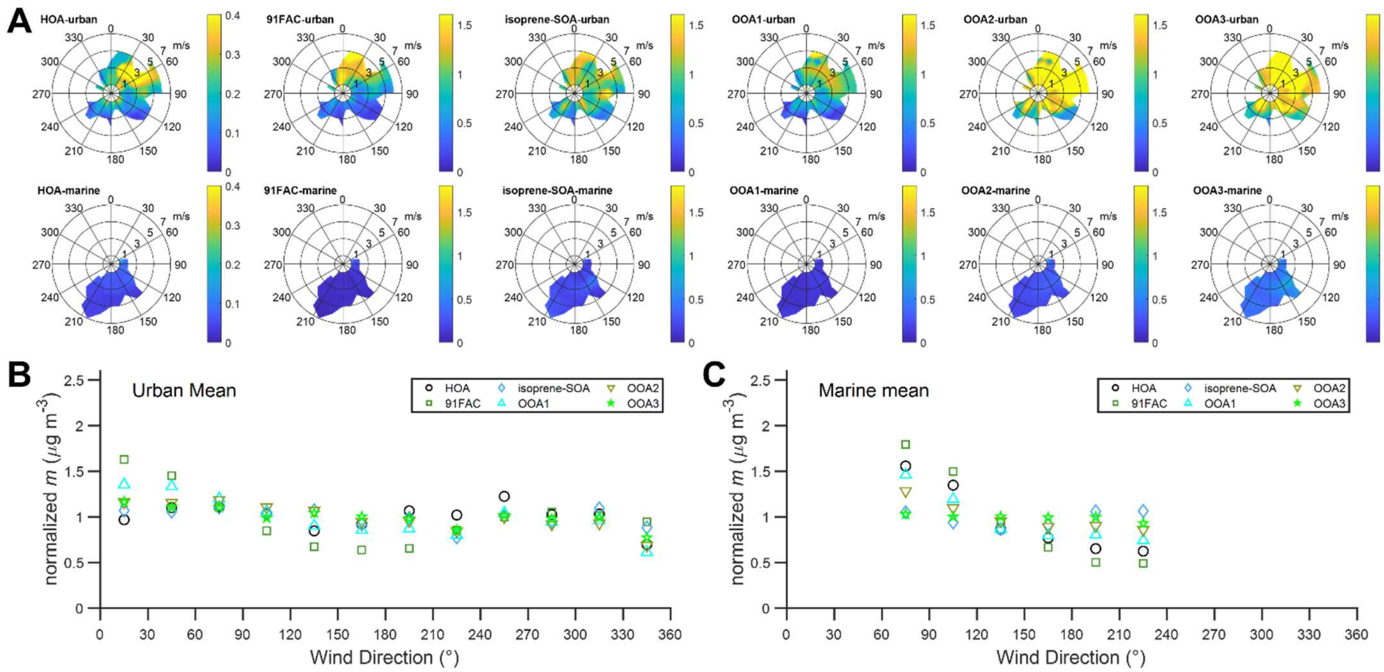

Figure S4. Wind pattern dependence of OA factors. (A) Wind-rose plots of OA factors in urban and marine air masses. Top row: urban. Bottom row: marine. **(B-C)** Normalized average mass concentration of OA factors as a function of wind direction in **(B)** urban and **(C)** marine air masses. OOA2 and OOA3 mass concentrations are largely independent of wind direction in urban and marine air masses.

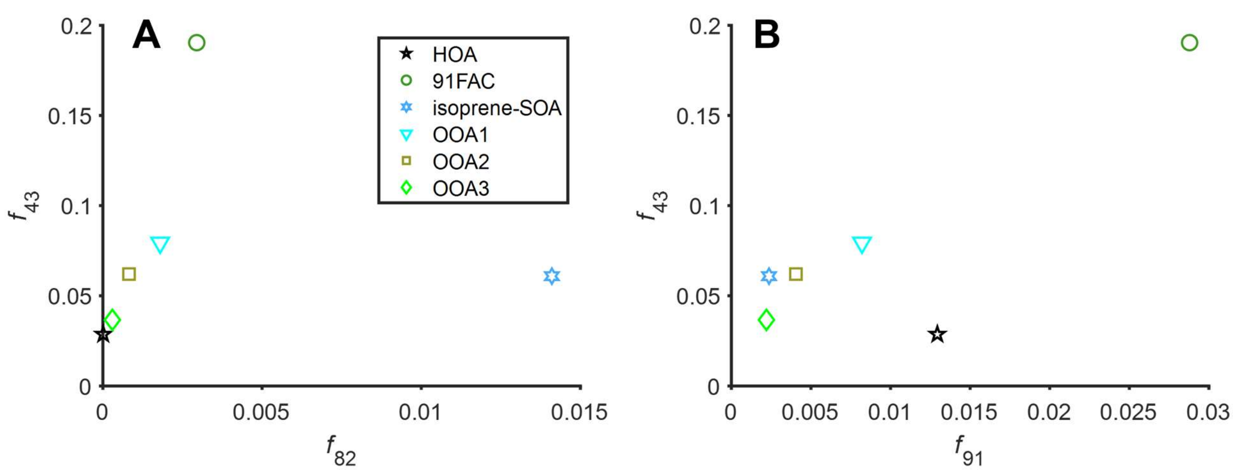

Figure S5. (A-B) f_{43} vs. f_{82} and f_{43} vs. f_{91} for all the PMF factors.

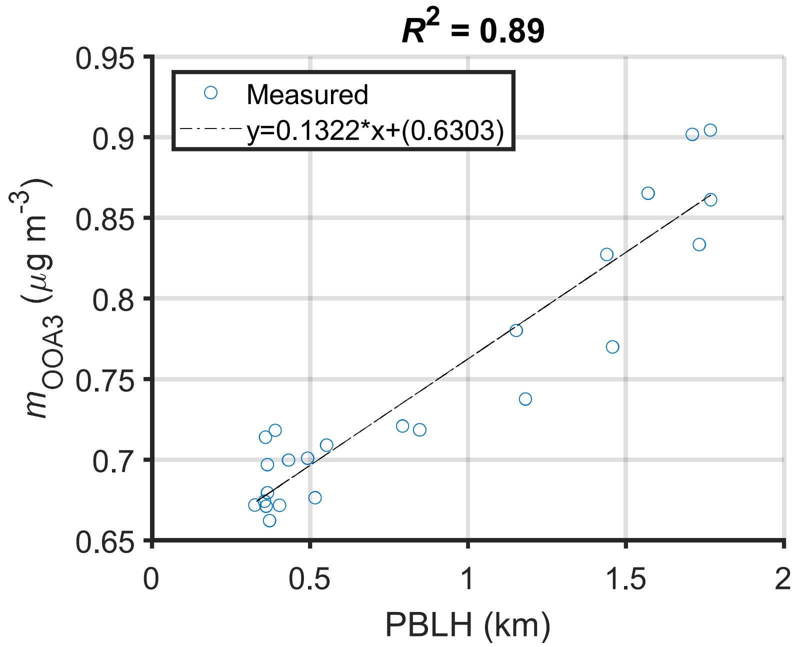

Figure S6. Diurnal variations of hourly averaged OOA3 mass concentrations vs. PBLH for unseparated air masses. The dashed line represents the least square linear regression.

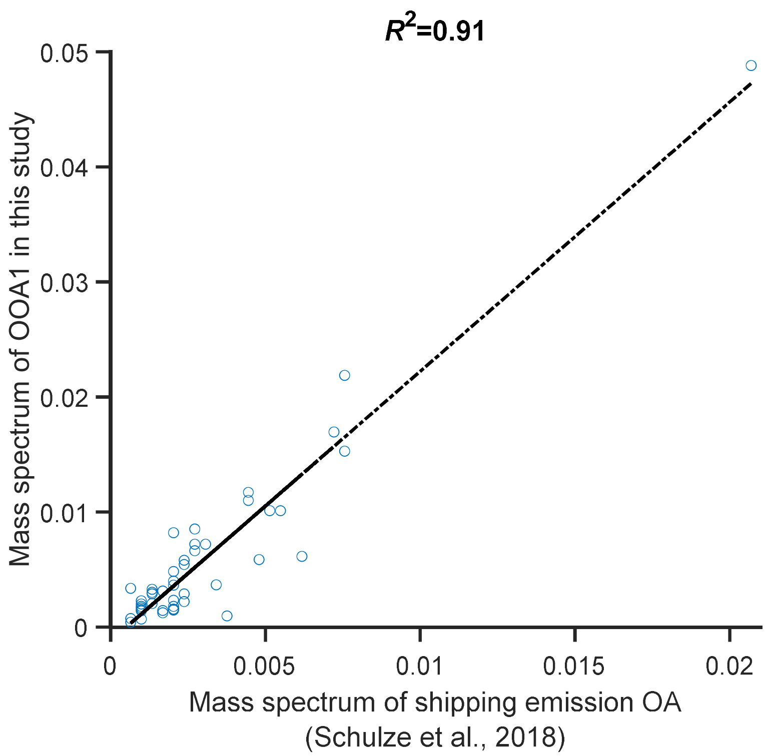

Figure S7. Correlation of the mass spectrum of OOA1 in this study with that of heavy shipping emission organics from Schulze et al. (2018).

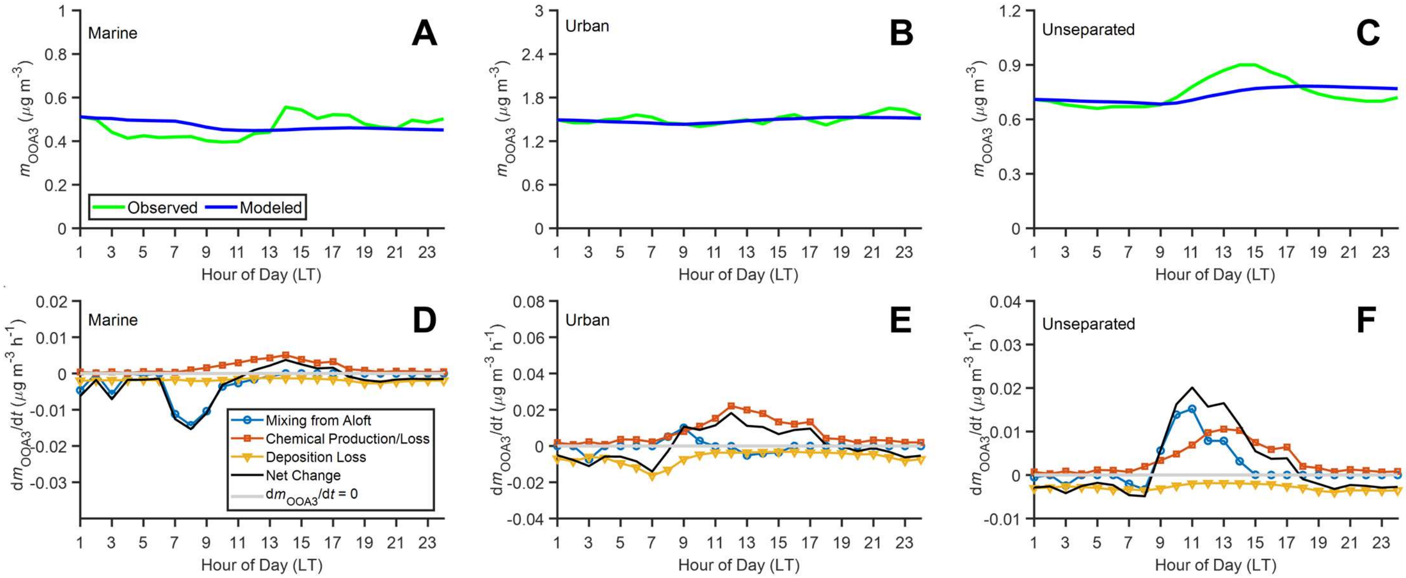

Figure S8. The sensitivity test of the 1-D box model (Same as Fig. 9 in the main text except that k_1, k_2, and k_3 are set to 2.5×10^{-12}, 5×10^{-13}, and 5×10^{-14} cm^3 molecule^{-1} s^{-1}, which are 50% lower than base values). (A, B, C) Diurnal variations of observed and modeled OOA3 mass concentrations in marine **(A)**, urban **(B)**, and unseparated **(C)** air masses from left to right. **(D, E, F)** Simulated contributions from different processes (mixing from aloft, chemical production/loss, deposition loss) and the net change rate of OOA3 within the PBLH in the marine **(D)**, urban **(E)**, and unseparated **(F)** air mass from left to right.

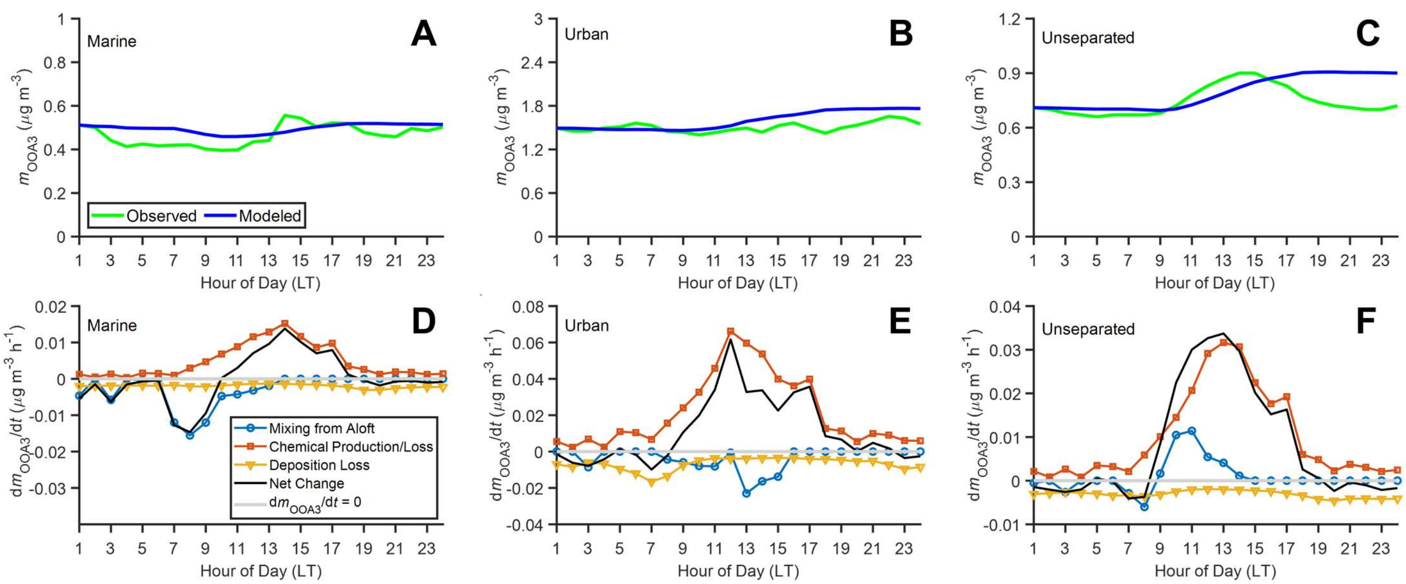

Figure S9. The sensitivity test of the 1-D box model (Same as Fig. 9 in the main text except that k_1, k_2, and k_3 are set to 7.5×10^{-12}, 1.5×10^{-12}, and 1.5×10^{-13} cm^3 molecule^{-1} s^{-1}, which are 50% higher than base values). (A, B, C) Diurnal variations of observed and modeled OOA3 mass concentrations in marine **(A)**, urban **(B)**, and unseparated **(C)** air masses from left to right. **(D, E, F)** Simulated contributions from different processes (mixing from aloft, chemical production/loss, deposition loss) and the net change rate of OOA3 within the PBLH in the marine **(D)**, urban **(E)**, and unseparated **(F)** air mass from left to right.

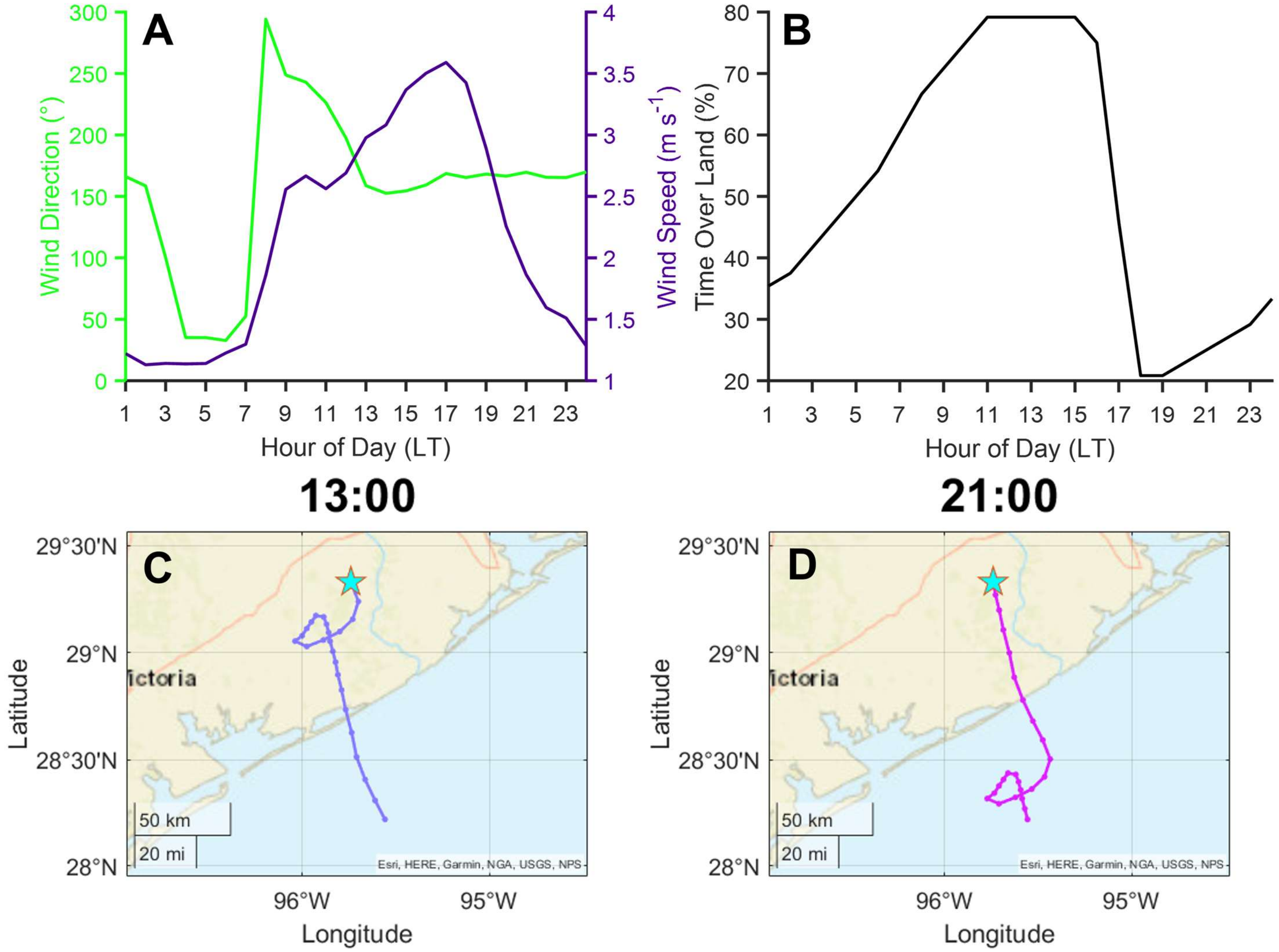

Figure S10. The circulation of land-sea/bay breezes increases the time of air mass over land and the fraction of urban air mass type observed at the ANC site midday. (A) Averaged diurnal variations of wind direction and wind speed over days with air mass changes during the IOP. **(B)** Percentage of time spent by the air mass over the land during the 24-hour period before arriving at the ANC site. The backward trajectories are derived from the diurnal variations of wind direction and speed averaged over days with air mass changes during IOP (i.e. Fig. S10A). **(C-D)** Derived backward trajectories at local times **(C)** 13:00 and **(D)** 21:00. ANC site is marked by the cyan star. .

Table S1. Instruments deployed at the ANC site during the TRACER IOP and measurements that are related to this study.

Measurement type	Instruments	Variable	Data available time (Local Time)	Time resolution
Meteorology	Vaisala automatic weather station	Surface wind speed, wind direction, air temperature, relative humidity, air pressure	05/29/2022-09/29/2022	1 min
Clouds	Ceilometer	Planetary boundary layer heights	06/30/2022-09/29/2022	16 s
Aerosol	Aerosol Chemical Speciation Monitor (ACSM)	Chemical compositions of aerosol particles	05/29/2022-09/29/2022	10 min
	Scanning Mobility Particle Sizer (SMPS)	Aerosol size distribution	05/29/2022-09/29/2022	5 min
	Condensation Particle Counter (CPC)	Total particle number concentration	05/29/2022-09/29/2022	1 min

Table S2. Comparison of OA mass spectra with those from earlier laboratory and field studies.

PMF Factors	Mass Spectra Comparison	Potential Sources	Potential Formation Pathways	ACSM Database numbers and References
HOA	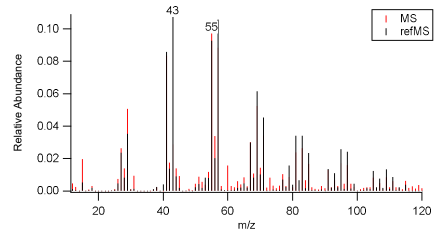	Road traffic (Barcelona, Spain)	Primary emission: Fossil fuel combustion dominated by diesel exhaust	256_DAURE campaign_2009_HOA; (Mohr et al., 2012)
	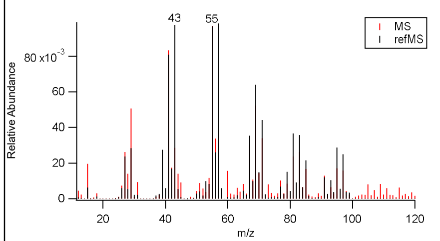	Road traffic (Riverside, USA)	Primary emission: Fuel and lubricating oil combustion	242_SOAR-1_Campaign_2005_HOA (Docherty et al., 2011)
91FAC	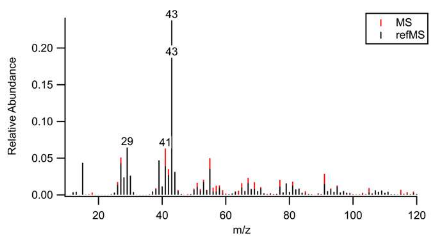	Lab experiment	Oxidation product of limonene by nitrate	380_Chamber limonene_Nitrate_AS_LIM-2 (Boyd et al., 2015)
	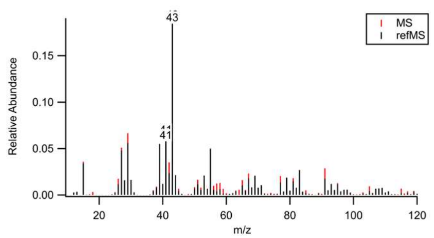	Lab experiment	Sequentially oxidation product of a-pinene and limonene by nitrate	382_Chamber α-pinene+limonene_Nitrate_ AS_dry_SEQ-1 (Takeuchi et al., 2022)
isoprene-SOA	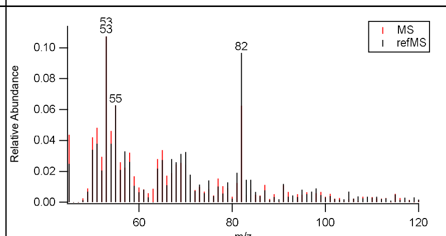	Tropical rainforest (Danum Valley, Borneo, Malaysia)	Isoprene oxidation	93_Borneo Rainforest_Fac82 (Robinson et al., 2011)
	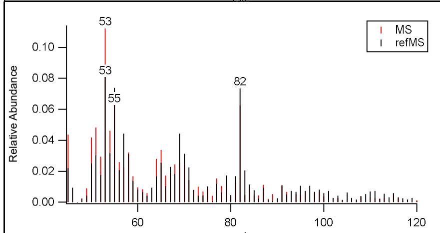	Forest (SE US forest)	isoprene oxidation	124_SOAS campaign_2013_IEPOX_SOA (Hu et al., 2015)

PMF Factors	Mass Spectra Comparison	Potential Sources	Potential Formation Pathways	ACSM Database numbers and References
OOA1	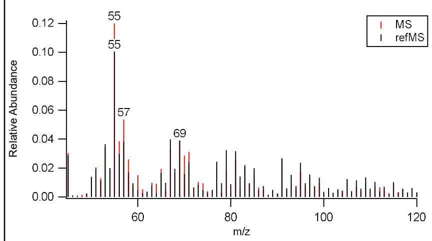	Urban area (Pasadena, CA, USA)	Photochemical formation of traffic emissions	292_CalNex campaign_2010_SV OOA (Hayes et al., 2013)
	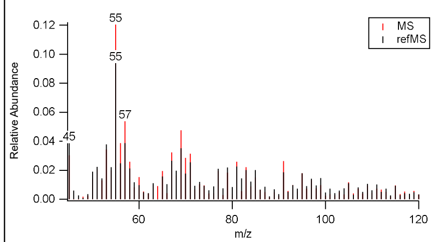	Urban area (Beijing, China)	VOC photochemical product	302_Beijing urban area_2011_LOOOA (Hu et al., 2016)
OOA2	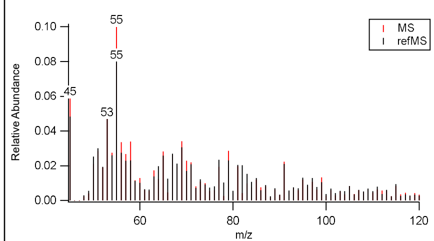	Urban area [Average of spectra in Beijing, Tokyo (summer), Pittsburgh, Riverside, New York City (summer), and Zurich]	VOC photochemical product	79_LVOOA_avg (Ng et al., 2011)
	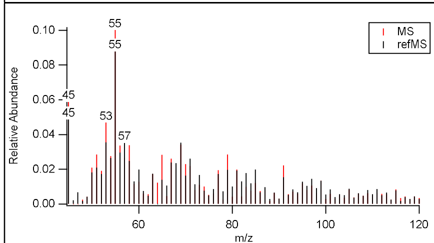	Downwind of pollution sources (Changdao island, China)	VOC photochemical product	299_Changdao island_2011_LVOO A (Hu et al., 2013)
OOA3	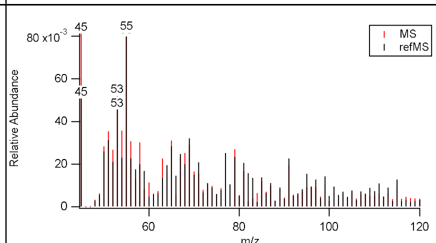	Urban area (Zurich, Switzerland)	Highly aged OOA; mass spectrum similar to fulvic acid	65_Zurich_summer_ 2005_OOA_I (Lanz et al., 2007)
	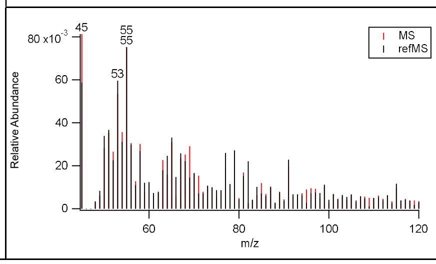	Urban area (Pittsburgh)	Highly aged OOA; well correlated to aged rural organic aerosols	64_Pittsburgh_OOA (Zhang et al., 2005)

Table S3. Correlation coefficients R^2 of OA factors with NO_3 and SO_4.

	NO_3	SO_4
HOA	0.28	0.07
91FAC	0.58	0.05
isoprene-SOA	0.40	0.36
OOA1	0.42	0.17
OOA2	0.42	0.24
OOA3	0.36	0.25

Table S4. Comparison of the mass concentrations of key aerosol components with those reported by prior studies in the Houston region.

	Location	Air mass	Total ($\mu g \cdot m^{-3}$)	Org ($\mu g \cdot m^{-3}$)	SO_4 ($\mu g \cdot m^{-3}$)	NH_4 ($\mu g \cdot m^{-3}$)	NO_3 ($\mu g \cdot m^{-3}$)	HOA ($\mu g \cdot m^{-3}$)	SOA ($\mu g \cdot m^{-3}$)
This study	Guy	Marine	3.55	1.42	1.47	0.50	0.16	0.07	1.29
		Urban	9.96	6.58	2.15	0.74	0.49	0.24	5.87
Yoon 2021	Manvel Croix							0.41	3.74
Dai 2019	Sugar Land		3.58	1.7	1.3	0.5	0.08	0.2	1.0
Wallace 2018	Manchester St.		10.8	5.5	2.5	1.3	1.5	0.67	1.93
Schulze 2018	Southwest of Galveston	Marine	3.82	0.7	2.4	0.7	0.02	0.05	0.64
		Urban	9.8	7.2	1.9	0.6	0.1	0.16	7.06
Al-Naiema 2018	Houston Ship Channel		2.86	1.14	1.29	0.4	0.03	0.42	0.72
Cleveland 2012	University of Houston		10.9	5.5	4.1	0.9	0.4	1.7	3.7

References

Boyd, C. M., Sanchez, J., Xu, L., Eugene, A. J., Nah, T., Tuet, W. Y., Guzman, M. I., and Ng, N. L.: Secondary organic aerosol formation from the β-pinene+NO_3 system: effect of humidity and peroxy radical fate, Atmospheric Chemistry and Physics, 15, 7497–7522, https://doi.org/10.5194/acp-15-7497-2015, 2015.

Docherty, K. S., Aiken, A. C., Huffman, J. A., Ulbrich, I. M., DeCarlo, P. F., Sueper, D., Worsnop, D. R., Snyder, D. C., Peltier, R. E., Weber, R. J., Grover, B. D., Eatough, D. J., Williams, B. J., Goldstein, A. H., Ziemann, P. J., and Jimenez, J. L.: The 2005 Study of Organic Aerosols at Riverside (SOAR-1): instrumental intercomparisons and fine particle composition, Atmospheric Chemistry and Physics, 11, 12387–12420, https://doi.org/10.5194/acp-11-12387-2011, 2011.

Hayes, P. L., Ortega, A. M., Cubison, M. J., Froyd, K. D., Zhao, Y., Cliff, S. S., Hu, W. W., Toohey, D. W., Flynn, J. H., Lefer, B. L., Grossberg, N., Alvarez, S., Rappenglück, B., Taylor, J. W., Allan, J. D., Holloway, J. S., Gilman, J. B., Kuster, W. C., de Gouw, J. A., Massoli, P., Zhang, X., Liu, J., Weber, R. J., Corrigan, A. L., Russell, L. M., Isaacman, G., Worton, D. R., Kreisberg, N. M., Goldstein, A. H., Thalman, R., Waxman, E. M., Volkamer, R., Lin, Y. H., Surratt, J. D., Kleindienst, T. E., Offenberg, J. H., Dusanter, S., Griffith, S., Stevens, P. S., Brioude, J., Angevine, W. M., and Jimenez, J. L.: Organic aerosol composition and sources in Pasadena, California, during the 2010 CalNex campaign, Journal of Geophysical Research: Atmospheres, 118, 9233–9257, https://doi.org/10.1002/jgrd.50530, 2013.

Hu, W., Hu, M., Hu, W., Jimenez, J. L., Yuan, B., Chen, W., Wang, M., Wu, Y., Chen, C., Wang, Z., Peng, J., Zeng, L., and Shao, M.: Chemical composition, sources, and aging process of submicron aerosols in Beijing: Contrast between summer and winter, Journal of Geophysical Research: Atmospheres, 121, 1955–1977, https://doi.org/10.1002/2015JD024020, 2016.

Hu, W. W., Hu, M., Yuan, B., Jimenez, J. L., Tang, Q., Peng, J. F., Hu, W., Shao, M., Wang, M., Zeng, L. M., Wu, Y. S., Gong, Z. H., Huang, X. F., and He, L. Y.: Insights on organic aerosol aging and the influence of coal combustion at a regional receptor site of central eastern China, Atmospheric Chemistry and Physics, 13, 10095–10112, https://doi.org/10.5194/acp-13-10095-2013, 2013.

Hu, W. W., Campuzano-Jost, P., Palm, B. B., Day, D. A., Ortega, A. M., Hayes, P. L., Krechmer, J. E., Chen, Q., Kuwata, M., Liu, Y. J., de Sá, S. S., McKinney, K., Martin, S. T., Hu, M., Budisulistiorini, S. H., Riva, M., Surratt, J. D., St. Clair, J. M., Isaacman-Van Wertz, G., Yee, L. D., Goldstein, A. H., Carbone, S., Brito, J., Artaxo, P., de Gouw, J. A., Koss, A., Wisthaler, A., Mikoviny, T., Karl, T., Kaser, L., Jud, W., Hansel, A., Docherty, K. S., Alexander, M. L., Robinson, N. H., Coe, H., Allan, J. D., Canagaratna, M. R., Paulot, F., and Jimenez, J. L.: Characterization of a real-time tracer for isoprene epoxydiols-derived secondary organic aerosol (IEPOX-SOA) from aerosol mass spectrometer measurements, Atmospheric Chemistry and Physics, 15, 11807–11833, https://doi.org/10.5194/acp-15-11807-2015, 2015.

Lanz, V. A., Alfarra, M. R., Baltensperger, U., Buchmann, B., Hueglin, C., and Prévôt, A. S. H.: Source apportionment of submicron organic aerosols at an urban site by factor analytical modelling of aerosol mass spectra, Atmospheric Chemistry and Physics, 7, 1503–1522, https://doi.org/10.5194/acp-7-1503-2007, 2007.

Mohr, C., DeCarlo, P. F., Heringa, M. F., Chirico, R., Slowik, J. G., Richter, R., Reche, C., Alastuey, A., Querol, X., Seco, R., Peñuelas, J., Jiménez, J. L., Crippa, M., Zimmermann, R., Baltensperger, U., and Prévôt, A. S. H.: Identification and quantification of organic aerosol from cooking and other sources in Barcelona using aerosol mass spectrometer data, Atmospheric Chemistry and Physics, 12, 1649–1665, https://doi.org/10.5194/acp-12-1649-2012, 2012.

Ng, N. L., Canagaratna, M. R., Jimenez, J. L., Zhang, Q., Ulbrich, I. M., and Worsnop, D. R.: Real-Time Methods for Estimating Organic Component Mass Concentrations from Aerosol Mass Spectrometer Data, Environ. Sci. Technol., 45, 910–916, https://doi.org/10.1021/es102951k, 2011.

Robinson, N. H., Hamilton, J. F., Allan, J. D., Langford, B., Oram, D. E., Chen, Q., Docherty, K., Farmer, D. K., Jimenez, J. L., Ward, M. W., Hewitt, C. N., Barley, M. H., Jenkin, M. E., Rickard, A. R., Martin, S. T., McFiggans, G., and Coe, H.: Evidence for a significant proportion of Secondary Organic Aerosol from isoprene above a maritime tropical forest, Atmospheric Chemistry and Physics, 11, 1039–1050, https://doi.org/10.5194/acp-11-1039-2011, 2011.

Schulze, B. C., Wallace, H. W., Bui, A. T., Flynn, J. H., Erickson, M. H., Alvarez, S., Dai, Q., Usenko, S., Sheesley, R. J., and Griffin, R. J.: The impacts of regional shipping emissions on the chemical characteristics of coastal submicron aerosols near Houston, TX, Atmospheric Chemistry and Physics, 18, 14217–14241, https://doi.org/10.5194/acp-18-14217-2018, 2018.

Takeuchi, M., Berkemeier, T., Eris, G., and Ng, N. L.: Non-linear effects of secondary organic aerosol formation and properties in multi-precursor systems, Nat Commun, 13, 7883, https://doi.org/10.1038/s41467-022-35546-1, 2022.

Zhang, Q., Alfarra, M. R., Worsnop, D. R., Allan, J. D., Coe, H., Canagaratna, M. R., and Jimenez, J. L.: Deconvolution and Quantification of Hydrocarbon-like and Oxygenated Organic Aerosols Based on Aerosol Mass Spectrometry, Environ. Sci. Technol., 39, 4938–4952, https://doi.org/10.1021/es048568l, 2005.